



# Growth responses of Norway spruce to weather variation across Finland over the past 60 years

Daesung Lee<sup>1</sup> , Helena Haakana<sup>2</sup>, Olli-Pekka Tikkasalo<sup>3</sup> , Harri Mäkinen<sup>4,\*</sup> 

Natural Resources Institute Finland (Luke), Latokartanonkaari 9, Helsinki 00790, Finland

## ARTICLE INFO

### Keywords:

Boreal forests  
Climate change  
Dendroecology  
*Picea abies* (L.) Karst.  
Radial increment

## ABSTRACT

To understand the effects of climate change on boreal forest productivity, it is crucial to examine tree growth variation and identify the climatic factors impacting it. Norway spruce (*Picea abies* (L.) Karst.) is a common and economically important tree species in Northern and Central Europe. Despite being sensitive to drought, it has been the preferred species for regeneration. Using an extensive tree-ring dataset collected as part of the Finnish National Forest Inventory, we identified the primary weather factors affecting annual radial growth variation in 4979 individual trees over the 1961–2023. We also analysed the spatial patterns of these relationships across Finland. This large-scale analysis revealed that high June temperatures promote tree growth at northern latitudes while the growth response to precipitation is weak. A clear south-north trend was observed in the weather-growth relationships. In southern and central Finland, warm, dry summers were detrimental to spruce growth. However, high June temperatures the previous year were negatively related to radial growth across the country. Furthermore, radial growth negatively responded to high winter temperatures. These results imply that temperature-induced water stress already limits spruce growth more severely and over a larger region than expected. It is likely that the anticipated benefits of global warming due to higher temperatures are diminished or negated by lower soil moisture availability or increased atmospheric evaporative demand.

## 1. Introduction

Ongoing global climate change is strongly influencing boreal forests. Summer temperature, the primary climatic driver of tree growth in Nordic forests, is expected to increase significantly (Ruosteenoja et al., 2020). Additionally, extreme weather events, including droughts, are expected to occur more frequent, particularly during spring and early summer. Higher temperatures may also lead to reduced snow accumulation due to decreased snowfall and earlier snowmelt (Serreze et al., 2000; Stone et al., 2002).

As temperature-limited ecosystems, climate change is commonly predicted to increase the growth and productivity of Nordic forests, and the growth response to precipitation has been weak (Salminen et al., 2009; Korpela et al., 2011; Fleischer et al., 2022). However, as the climate changes, the factors limiting tree growth are also changing, and

the interaction between rising temperatures and increasing precipitation heterogeneity is placing trees under greater water stress (Allen et al., 2015; Ruiz-Pérez and Vico, 2020). Previous results have indicated that water availability and drought may also influence tree growth at high northern latitudes (Henttonen et al., 2014). Furthermore, National Forest Inventory (NFI) results from the Nordic countries suggest that warm summers in recent years have reduced forest growth (Mäkinen et al., 2022; Laudon et al., 2024).

Norway spruce (*Picea abies* (L.) Karst.) (hereafter spruce) is one of the most common and economically important tree species in Northern and Central Europe. It has been the preferred species for regeneration in the Nordic countries (Lidskog and Sjödin, 2014; Lodin et al., 2017). Even though spruce is a drought-sensitive species, it is also commonly planted on suboptimal, dryish sites, largely because pine saplings are frequently damaged by large populations of moose and deer (Wallgren et al., 2013;

\* Corresponding author.

E-mail addresses: [daesung.lee@luke.fi](mailto:daesung.lee@luke.fi) (D. Lee), [helena.haakana@luke.fi](mailto:helena.haakana@luke.fi) (H. Haakana), [olli-pekka.tikkasalo@luke.fi](mailto:olli-pekka.tikkasalo@luke.fi) (O.-P. Tikkasalo), [harri.makinen@luke.fi](mailto:harri.makinen@luke.fi) (H. Mäkinen).

<sup>1</sup> [orcid.org/0000-0003-1586-9385](https://orcid.org/0000-0003-1586-9385)

<sup>2</sup> [orcid.org/0000-0002-4830-800X](https://orcid.org/0000-0002-4830-800X)

<sup>3</sup> [orcid.org/0000-0003-1729-6349](https://orcid.org/0000-0003-1729-6349)

<sup>4</sup> [orcid.org/0000-0002-1820-6264](https://orcid.org/0000-0002-1820-6264)

<https://doi.org/10.1016/j.foreco.2026.123967>

Received 24 April 2026; Received in revised form 29 May 2026; Accepted 30 May 2026

Available online 7 June 2026

0378-1127/© 2026 The Author(s). Published by Elsevier B.V. This is an open access article under the CC BY license (<http://creativecommons.org/licenses/by/4.0/>).

Nevalainen et al., 2016). Spruce growth in a changing climate shows divergent trends based on latitude and moisture availability. While higher temperatures promote growth in northern, high-latitude regions, climate change threatens the viability of spruce in southern and lower-elevation areas due to drought and heat stress (Kellomäki et al., 2018; Matkala et al., 2021). Spruce is susceptible to drought due to its shallow root system and long evaporating canopy (Mauer et al., 2008; Lévesque et al., 2013). Droughts have been shown to limit the growth of spruce trees and result in mortality in southern Finland as well (Mäkinen et al., 2001; Jyske et al., 2010).

To understand the effects of climate change on the productivity of boreal forests, it is crucial to examine the interactions between increasing temperature and altered water availability. Analysing tree rings provides a means of investigating variability in tree growth and revealing the varying climatic factors that have impacted growth over time. Extensive tree-ring data sets that have been systematically sampled as part of NFIs in different countries have been used to study growth-climate relationships (e.g., Henttonen et al., 2014; Aldea et al., 2023; Merlin et al., 2024). NFI data represent forests across the full ecological gradient of the region, unlike targeted sampling approaches, such as sampling old trees from ecologically marginal sites (cf., Klesse et al., 2018).

In previous studies, the growth-climate relationships of spruce and Scots pine (*Pinus sylvestris* L.) were analysed along a latitudinal gradient from southern to northern Finland using NFI data (Henttonen et al., 2014, 2017). The results revealed gradual changes in growth responses along the south-north gradient. In these studies, the approach to studying the climatic signal in tree rings has been to relate weather data to regional average indices calculated for the boreal biogeographic subzones or for NFI sampling regions. However, the climatic signal in aggregated tree-ring chronologies may be obscured because regional averaging fails to capture local variation in weather conditions and the responses of individual trees. For this reason, in this study we calculated climate-growth relationships separately for the ring-width time series of each individual tree (cf., Aldea et al., 2023; Merlin et al., 2024).

The objectives of this study were to identify the main weather factors influencing the annual radial growth variation of spruce on mineral soils, and to analyse the spatial patterns of these relationships across Finland. We also examined whether the relationship between weather and growth varies at different levels of site fertility.

## 2. Materials and methods

### 2.1. Study area and NFI data

The study covered almost the entire continental part of Finland, spanning four vegetation zones (Fig. 1) (Ahti et al., 1968). The northernmost part of Lapland, mainly characterised by open fells and sparse pine or silver birch (*Betula pendula* Roth.) forests, was excluded from the study. The Finnish NFI uses a systematic cluster sampling design comprising permanent and temporary sample plots. In each NFI cycle, approximately one-fifth of the sample plots are measured annually. The country is divided into six sampling regions, each with a slightly different design adapted to the large-scale variation in forest characteristics from south to north (Tomppo et al., 2011). The Åland Islands and northernmost Lapland are special sampling regions where all plots are measured within a single year of an inventory cycle. The proportion of permanent clusters has increased from 25% in NFI1–60% in NFI2, and further to 80% in NFI3 (Korhonen et al., 2017, 2021, 2024). In this study, we used data measured on temporary sample plots during three consecutive NFI cycles: NFI1 (2009–2013), NFI2 (2014–2018), and NFI3 (2019–2023).

Stand-level variables recorded for NFI sample plots include information on land use, administrative status, growing stock, site and soil conditions, damage and forest management operations. These variables are typically assessed within the 0.25-hectare area surrounding the plot

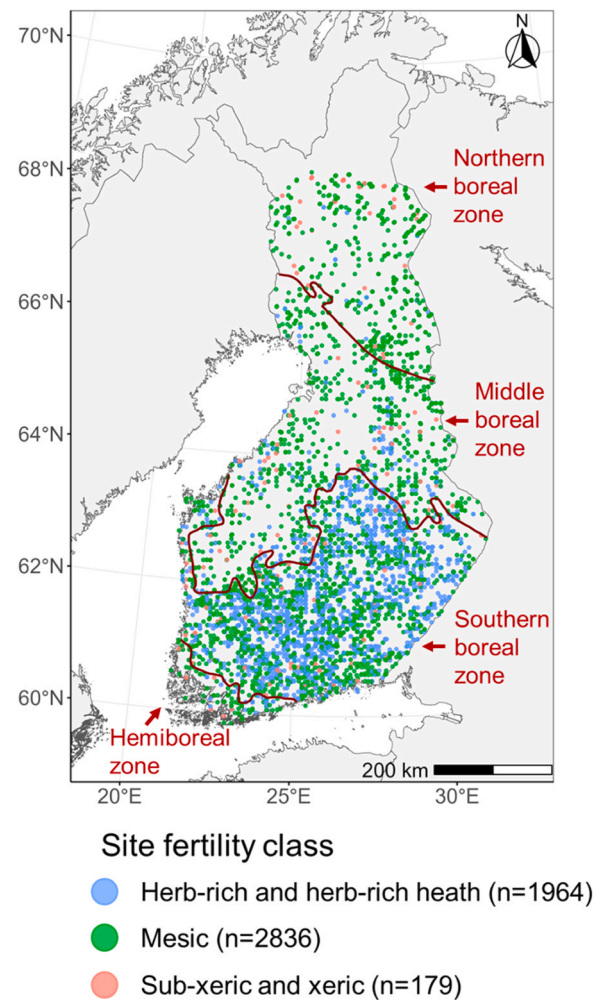


Fig. 1. Distribution of NFI11, NFI12 and NFI13 temporary plots on mineral soil used in this study, overlaid with vegetation zones. The colors indicate site fertility classes: fertile and relatively fertile herb-rich and herb-rich heath sites; medium fertile mesic heath sites; and relatively infertile and infertile sub-xeric and xeric heath sites; n is the number of plots in each site fertility class.

center. If a plot intersects two or more stands, each stand is described separately. The site variables used for data selection and categorisation were: (i) main site type, which classifies forest land as either mineral soils or peatlands, and (ii) site fertility type, which groups forests into eight classes based on fertility and wood production capacity within vegetation zones (Lehto and Leikola, 1987; Hotanen et al., 2008). Detailed information on field measurements and variable classifications is provided in the NFI field manual (Korhonen et al., 2024, S3).

In NFI12 and NFI13, all trees taller than 1.3 m were measured within concentric circular plots with radius of 4 or 9 m depending on tree size. Trees smaller than 4.5 cm in diameter were measured using a Bitterlich relascope plot with a basal area factor of 1.5 m<sup>2</sup>/ha (Bitterlich, 1984; Korhonen et al., 2024). In NFI11, the plots were Bitterlich relascope plots with maximum radius of 9, 12.52 or 12.45 m (Korhonen et al., 2017). A sub-sample of tallied trees was measured in greater detail to estimate their volume and increment. Sample trees were selected using the probability proportional to size (PPS) sampling method. On temporary plots, sample trees were cored at breast height (1.3 m) from one side of the stem to the pith using a Suunto increment borer (Suunto, Finland). In the laboratory, the cores were scanned, and annual ring widths were measured using WinDENDRO™ software (Regent Instruments, Quebec, Canada).

## 2.2. Weather variables

Daily weather data from 1961 to 2023 were obtained from the weather database, provided by the Finnish Meteorological Institute (FMI). The dataset includes daily mean, maximum and minimum temperature, global radiation intensity, water vapor pressure and precipitation. Among all available weather variables, the six most representative and least intercorrelated variables were selected for analysis: mean daily average temperature ( $^{\circ}\text{C}$ ) in a month ( $T_{\text{avg}}$ ), 1st percentile of minimum daily temperatures ( $^{\circ}\text{C}$ ) in a month ( $T_{\text{min}}$ ), 99th percentile of maximum daily temperatures ( $^{\circ}\text{C}$ ) in a month ( $T_{\text{max}}$ ), precipitation sum (mm) in a month ( $\text{Prec}_{\text{sum}}$ ), mean daily water vapor pressure deficit (kPa; calculated from water vapor pressure and  $T_{\text{avg}}$ ) in a month (VPD), and mean daily global radiation intensity ( $\text{kJ m}^{-2} \text{day}^{-1}$ ) in a month (GlobR). The daily data were aggregated to monthly, annual, and growing season (May–August or April–September) scales using arithmetic means.

The original data were available at a spatial resolution of  $10 \text{ km} \times 10 \text{ km}$  for the period 1961–11/2016 and at a resolution of  $1 \text{ km} \times 1 \text{ km}$  for 12/2016–2023. The  $1 \text{ km} \times 1 \text{ km}$  data were aggregated to match the  $10 \text{ km} \times 10 \text{ km}$  resolution by assigning each  $1 \text{ km}$  cell to the geographically nearest  $10 \text{ km}$  grid cell (target coordinate). All  $1 \text{ km}$  cells with a grid centre below a distance of  $D \leq \sqrt{(2 \times (5 \text{ km})^2)}$  from a target coordinate were selected. For each target grid cell, the mean value was computed for each weather variable across all selected  $1 \text{ km}$  cells, except for  $T_{\text{min}}$  and  $T_{\text{max}}$ , which were aggregated using the 1st and 99th percentiles, respectively. In addition, we calculated the standardised precipitation index (SPI) using the Python package climate-indices (Adams, 2017). SPI was computed using the gamma function method at six different time scales (1-, 2-, 3-, 6-, 12- and 24-month intervals) based on total monthly precipitation.

All weather data were stored in netCDF format and imported into R for analysis using the *ncdf4* package. To integrate the weather information with the NFI plots, a spatial join was performed using the *st\_nearest\_feature()* function from the *sf* package, which assigned each NFI plot to the weather data from the nearest grid cell. Finally, all spatial

maps were displayed using the EPSG:3067 ETRS89 / TM35FIN (E, N) coordinate reference system.

Descriptive statistics of the weather variables examined in this study for June and February are presented in Table 1 to illustrate the differences among the vegetation zones. The most representative temperature- and moisture-related variables of these two months are also shown as line plots for the period 1961–2023, highlighting their fluctuations and long-term trends (Fig. 2).

## 2.3. Compilation of tree-ring indices

We used ring-width data from dominant and co-dominant spruce sample trees growing in productive forests (annual growth rate  $\geq 1 \text{ m}^3 \text{ ha}^{-1} \text{ yr}^{-1}$ ) on undrained mineral soil. Trees on drained mineral soil were excluded to avoid the confounding effect of ditching on tree growth. We also excluded trees growing on infertile barren mineral soils, rocky and sandy soils and alluvial land (site fertility classes six and seven) (Korhonen et al., 2024, S3). To ensure a sufficient sample size within each vegetation zone, the hemiboreal and southern boreal zones were combined because the hemiboreal zone covers only a small area along the southwest coast (Fig. 1). For quality assurance, we only included sample trees with a diameter greater than 4.5 cm and with at least ten measured annual rings. A total of 11,844 sample trees with annual ring-width data were available for the period 1960–2023. The length of the tree-ring width (TRW) series ranged from 10 to 63 years (Fig. 2).

To remove the effects of tree size, age, competition and management on annual growth variation, the TRW measurements were standardised into ring-width indices (RWI) using the R package *dplR* (Bunn, 2008; Bunn et al., 2025). Detrending was performed using the cubic smoothing spline method with a 50% frequency cutoff in 30 years. The series were not pre-whitened to remove autocorrelation. To ensure a correct dating, we discarded RWI series that did not meet the following quality criteria: 1) RWIs were normally distributed; 2) the expressed population signal (EPS) was greater than 0.85 among the 30 geographically nearest series, and 3) the mean inter-series correlation was greater than 0.4 among the same 30 nearest series (cf., Aldea et al., 2023; Merlin et al., 2024). The

**Table 1**

Summary statistics of the main weather variables analysed in this study by vegetation zone for June and February (1961–2023). They were calculated using the 1st–99th percentile range of all observations from 1961 to 2023.

Variable	June				February			
	Mean	S.D.	Min.	Max.	Mean	S.D.	Min.	Max.
<i>Southern boreal and hemiboreal zone</i>								
$T_{\text{avg}}$	14.40	1.77	8.93	18.47	−7.71	4.38	−19.49	0.17
$T_{\text{min}}$	2.55	2.10	−2.82	7.62	−24.53	6.46	−38.78	−9.16
$T_{\text{max}}$	26.52	2.51	19.77	31.67	2.56	2.53	−5.29	8.26
$\text{Prec}_{\text{sum}}$	53.41	25.49	7.00	128.00	27.99	17.26	1.00	83.53
VPD	0.58	0.13	0.31	0.92	0.04	0.01	0.01	0.09
GlobR	20312.6	2535.7	12915.3	26856.6	2623.97	524.7	1170.6	4284.5
$\text{SPI}_{1\text{-month}}$	0.02	0.94	−2.66	2.04	0.03	0.92	−2.36	2.04
<i>Middle boreal zone</i>								
$T_{\text{avg}}$	13.35	1.83	8.63	18.46	−9.37	4.30	−19.49	0.17
$T_{\text{min}}$	1.20	1.91	−2.82	7.60	−27.18	5.73	−38.78	−9.17
$T_{\text{max}}$	25.99	2.60	19.77	31.67	2.01	2.54	−5.29	8.26
$\text{Prec}_{\text{sum}}$	55.02	25.02	7.00	128.00	26.94	17.32	1.00	83.50
VPD	0.55	0.12	0.31	0.92	0.03	0.01	0.01	0.09
GlobR	19904.9	2471.3	12912.2	26854.5	2208.9	496.6	1168.1	4263.0
$\text{SPI}_{1\text{-month}}$	0.00	0.91	−2.66	2.04	0.04	0.94	−2.35	2.03
<i>Northern boreal zone</i>								
$T_{\text{avg}}$	11.74	1.79	8.63	16.36	−11.85	3.70	−19.49	−1.54
$T_{\text{min}}$	0.06	1.51	−2.82	5.53	−30.50	4.32	−38.78	−13.36
$T_{\text{max}}$	25.00	2.63	19.77	31.57	0.96	2.46	−5.30	7.32
$\text{Prec}_{\text{sum}}$	55.59	24.83	7.00	128.00	25.64	16.90	1.00	83.00
VPD	0.52	0.11	0.31	0.91	0.03	0.01	0.01	0.09
GlobR	18665.0	2320.1	12912.2	26843.3	1690.6	392.2	1168.0	3469.1
$\text{SPI}_{1\text{-month}}$	0.01	0.94	−2.66	2.04	−0.02	0.96	−2.36	2.04

Abbreviations:  $T_{\text{avg}}$  = mean daily average temperature ( $^{\circ}\text{C}$ ) in a month;  $T_{\text{min}}$  = 1st percentile of minimum daily temperatures ( $^{\circ}\text{C}$ ) in a month;  $T_{\text{max}}$  = 99th percentile of maximum daily temperatures ( $^{\circ}\text{C}$ ) in a month;  $\text{Prec}_{\text{sum}}$  = precipitation sum (mm) in a month; VPD = mean daily water vapor pressure deficit (kPa) in a month; GlobR = mean daily global radiation intensity ( $\text{kJ m}^{-2} \text{day}^{-1}$ ) in a month;  $\text{SPI}_{1\text{-month}}$  = standardised precipitation index based on total monthly precipitation (mm/month).

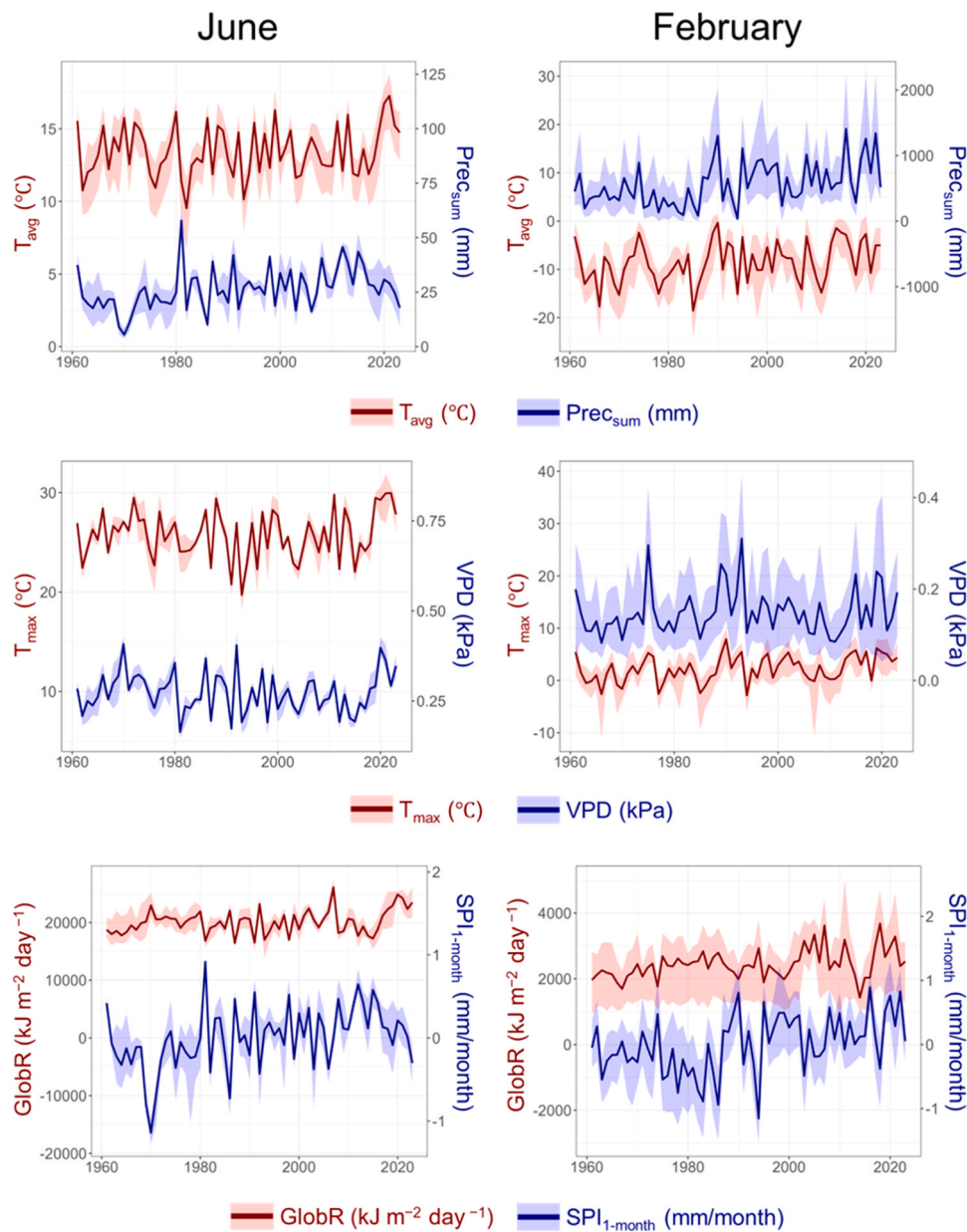


**Fig. 2.** Average weather variables (1961–2023) for June and February on the plots included in the dataset. The solid lines represent the arithmetic mean for each year, and the shaded areas depict the 1st–99th percentile range of all observations in each year. Abbreviations:  $T_{avg}$  = mean daily average temperature ( $^{\circ}\text{C}$ ) in a month;  $T_{max}$  = 99th percentile of maximum daily temperature ( $^{\circ}\text{C}$ ) in a month;  $Prec_{sum}$  = precipitation sum (mm) in a month; VPD = mean daily water vapor pressure deficit (kPa) in a month; GlobR = mean daily global radiation intensity ( $\text{kJ m}^{-2} \text{day}^{-1}$ ) in a month;  $SPI_{1\text{-month}}$  = standardised precipitation index based on total monthly precipitation (mm/month).

final dataset used in the analyses included 4979 RWI series (Fig. 3). The number of plots with one sample tree was 82%, 16% had two and 2% had three or more.

#### 2.4. Growth responses to the 1961–2023 weather variation

The relationship between monthly weather variables and every individual RWI series were analysed using Spearman's rank correlation coefficient ( $\rho$ ), making the correlation free from assumptions such as normality and linearity, and enabling nonlinear but monotonic relationships to be captured. Spearman's rank correlation coefficient ( $\rho$ ) was calculated for each individual tree over the entire time series available over the 1961–2023 period. The analysis was restricted to the previous year (i.e., one year before ring formation) and the current year (i.e., the year of ring formation). The weather variables used in the

correlation analysis were:  $T_{avg}$ ,  $T_{max}$ ,  $T_{min}$ ,  $Prec_{sum}$ , VPD, GlobR,  $SPI_{1\text{-month}}$ ,  $SPI_{2\text{-month}}$ ,  $SPI_{3\text{-month}}$ ,  $SPI_{6\text{-month}}$ ,  $SPI_{12\text{-month}}$ , and  $SPI_{24\text{-month}}$ . We also tested the correlation coefficients using weather data from different time ranges; e.g., monthly weather variables, May–August growing season, April–September growing season, and yearly weather data.

To demonstrate the dominant effect of weather variation on tree growth, we identified the six variables with the greatest number of significant Spearman's rank correlation coefficients ( $\rho$ ) ( $p < 0.05$ ). We then plotted the significant correlation coefficients on maps based on the plot locations to show the spatial variability of the growth–climate relationships across Finland. To further describe this variability, we examined how the correlation coefficients of the top six variables changed with the long-term mean June temperature of each plot. In the scatter plots showing site fertility classes, we fitted a simple regression line and used dummy variables in the intercept and slope to separate the

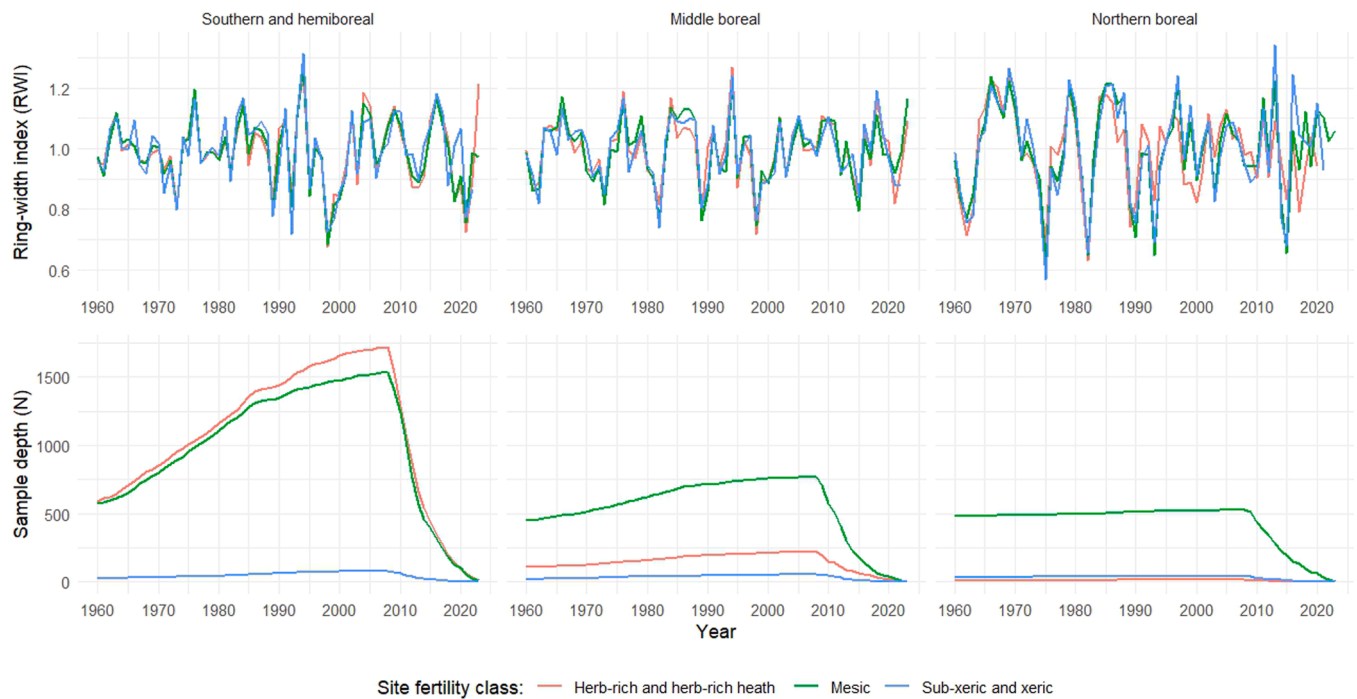


Fig. 3. Average annual ring-width indices (RWI) and sample depth (N) according to forest vegetation zone and site fertility class in the NFI11–NFI13 dataset.

fertility classes.

Finally, distributions of tree age at breast height were calculated to compare age differences between trees exhibiting significant and non-significant correlations between ring-width indices (RWI) and June temperatures in the previous year. The aim was to test whether trees showing significant correlations with previous-year summer temperatures were older, potentially indicating greater cone production in mature stands. We also conducted an analysis examining tree age distributions across different sample sizes (i.e., the number of rings in the core in five-year intervals), grouping them according to statistical significance (significant negative, non-significant, significant positive). The analysis showed that the age distributions were similar within each sample size group, regardless of statistical significance (Supplementary Fig. S1).

### 3. Results

The correlations of the ring-width indices (RWI) were stronger with the weather variables of individual months than with the averaged yearly or growing season (May–August or April–September) variables. Therefore, the results are reported based on monthly variables. Of all the months in the current and previous years, the RWIs of individual trees were primarily correlated with June weather variables of the current year (Table 2). The maximum daily temperature in June of the current summer had the highest number of significant correlations with RWIs, followed by the mean daily average temperature in June of the previous year. Additionally, the water vapor pressure deficit, global radiation intensity and precipitation index in June of the current year exhibited a high number of significant correlations. Moreover, nearly 20% of the correlations with average February temperatures of the preceding winter were significant.

The correlations of individual tree RWIs with the top weather variables exhibited clear spatial patterns across Finland (Fig. 4). In southern and central Finland, almost all of the significant Spearman’s rank correlation coefficients with the maximum daily temperature in current summer June were negative, whereas in the north, they were positive (Fig. 4a). The spatial variability of water vapor pressure deficit and global radiation intensity in current June was similar to that of June

Table 2

Number of significant positive and negative correlations ( $p < 0.05$ ) between the ring-width index series of individual trees and the top six weather variables, alongside their time periods. A total of 4979 trees were used to calculate Spearman’s rank correlations. The subscript “prev” in the period column refers to the previous year.

Climatic variable	Period	Number of trees with a significant correlation			
		Total	Positive correlation	Negative correlation	Percentage
$T_{max}$	June	1777	297	1480	35.69%
$T_{max}$	June <sub>prev</sub>	1096	14	1082	22.01%
VPD	June	1001	389	612	20.10%
$T_{avg}$	February	954	77	877	19.16%
GlobR	June	632	216	416	12.69%
SPI <sub>1-month</sub>	June	620	541	79	12.45%

Note:  $T_{max}$  = 99th percentile value of the maximum daily temperature ( $^{\circ}\text{C}/\text{day}$ ) in a given period (e.g., month); VPD = mean daily water vapor pressure deficit (kPa) in a given period;  $T_{avg}$  = mean daily average temperature ( $^{\circ}\text{C}/\text{day}$ ) in a given period; GlobR = mean daily global radiation intensity ( $\text{kJ m}^{-2} \text{day}^{-1}$ ) in a given period; SPI<sub>1-month</sub> = standardised precipitation index based on total precipitation during one month (mm/month).

temperature, i.e., negative correlations in southern and central Finland and positive correlations in the north (Fig. 4c and 4e). Additionally, the precipitation index in current June showed a similar, yet opposite, spatial trend, i.e., high June precipitation was related to higher increment indices in southern parts of the country and lower increments in the north (Fig. 4 f). In contrast, maximum daily temperatures in June of the previous year and mean daily temperatures in February of the current year were negatively correlated with RWIs across the whole country (Figs. 4b and 4d).

We observed clear differences in the climate-growth relationships among the vegetation zones (Fig. 5). Spearman’s rank correlation coefficients of maximum daily temperature, water vapor pressure deficit and global radiation intensity in current summer June decreased from positive to negative as the mean June temperature increased (Figs. 5a, 5c, and 5e), while the opposite was observed for the precipitation index

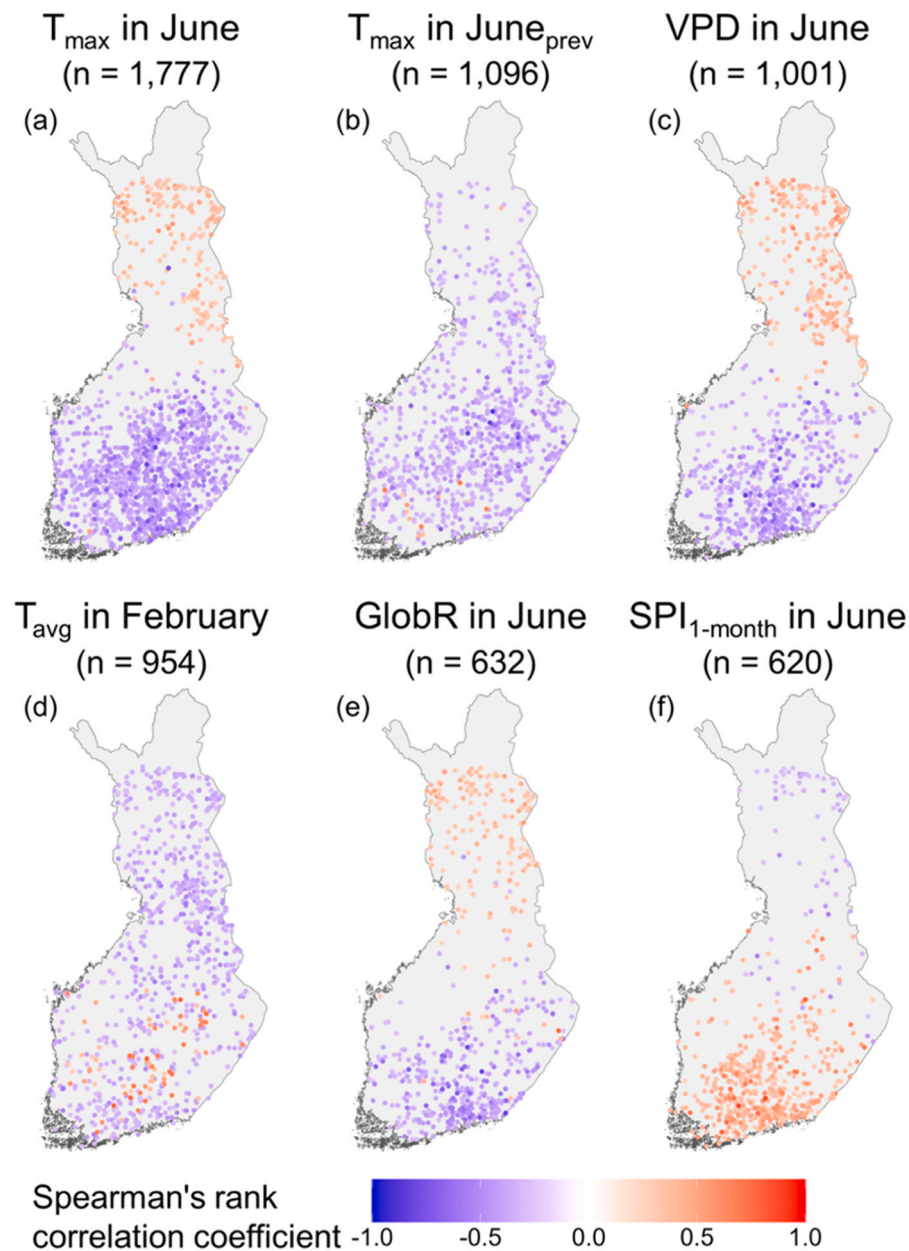


**Fig. 4.** Significant Spearman's rank correlation coefficients ( $p < 0.05$ ) between the top six weather variables and the ring-width indices (RWI) of individual trees based on NFI plot locations. Symbol  $n$  shows the number of significant correlations out of 4979 trees. Abbreviations:  $T_{\max}$  = 99th percentile of maximum daily temperature ( $^{\circ}\text{C}$ ) in a month; VPD = mean daily water vapor pressure deficit (kPa) in a month;  $T_{\text{avg}}$  = mean daily average temperature ( $^{\circ}\text{C}$ ) in a month; GlobR = mean daily global radiation intensity ( $\text{kJ m}^{-2} \text{day}^{-1}$ ) in a month;  $\text{SPI}_{1\text{-month}}$  = standardised precipitation index based on total monthly precipitation (mm/month).

(Fig. 5, plot f). Thus, in the northern boreal zone, the correlation coefficients of maximum daily temperature, water vapor pressure deficit and global radiation intensity were primarily positive, whereas in the hemiboreal and southern boreal zones, they were negative (Figs. 5a, 5c, and 5e). The correlations switched from positive to negative (or from negative to positive) for the precipitation index) at a mean June temperature of approximately  $13^{\circ}\text{C}$  in the middle boreal zone in the central part of the country. In the northern and central boreal zones, high February temperatures were negatively correlated with RWIs, whereas in the southern boreal zone, the correlations ranged from negative to positive (Fig. 5). There were no clear differences in the correlations between the average June temperatures of the previous year and RWIs across the vegetation zones; they were predominantly negative in all zones (Fig. 5b).

Examining the correlation coefficients between the top weather

variables and RWIs, and their trends according to the long-term average June temperature, revealed no major differences between the site fertility classes (Fig. 6). Finally, the distributions of tree age at breast height showed that, on average, trees with significant negative correlations between maximum daily temperatures in June the previous year and RWIs were older (92.6 years) than trees with non-significant correlations (71.6 years) or significant positive correlations (59.9 years) (Fig. 7).

#### 4. Discussion

This study presents a spatial approach to analysing variation in radial growth and its climatic drivers across Finland. The results showed that weather in June is an important factor influencing spruce growth in the Nordic countries (cf., Mäkinen et al., 2000; Andreassen et al., 2006;

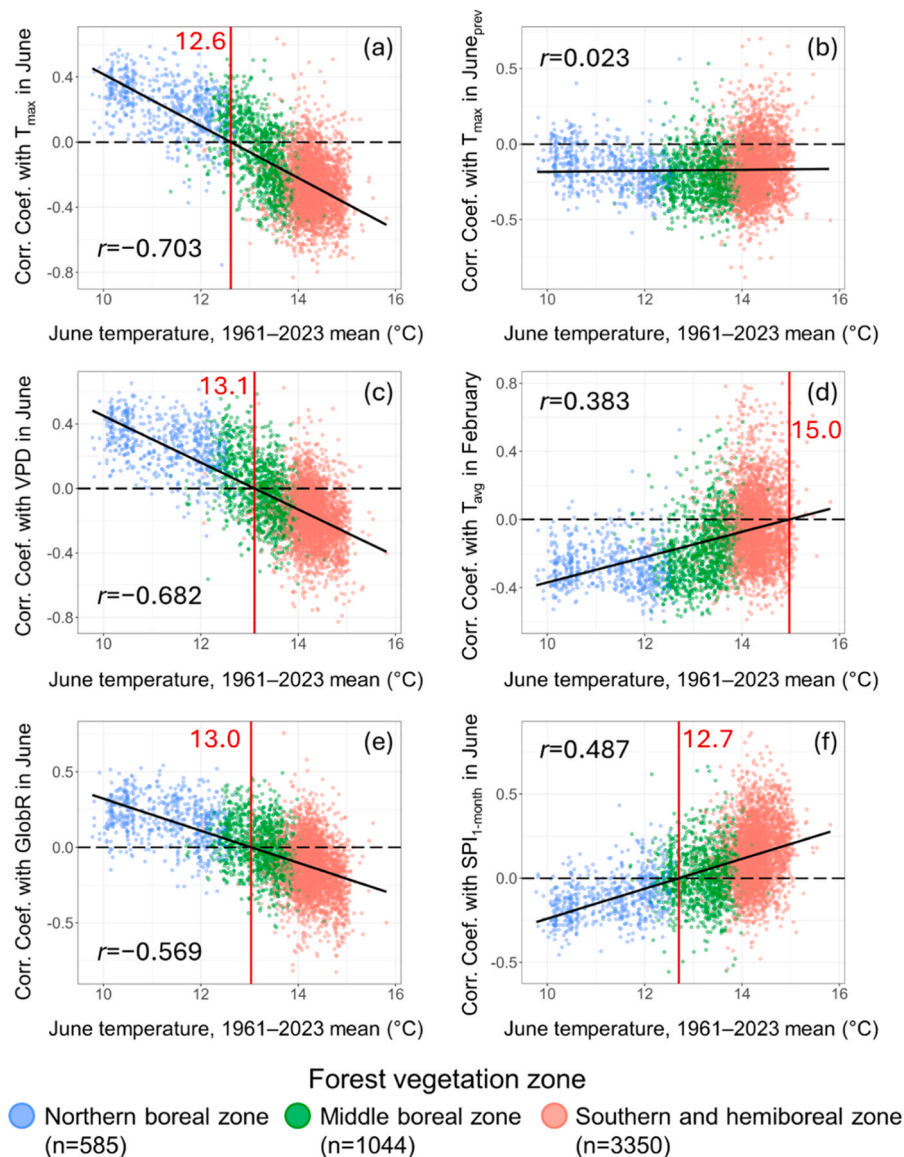


**Fig. 5.** Spearman's rank correlation coefficients between the top six weather variables and the ring-width indices (RWI) of individual trees, plotted against the long-term mean (1961–2023) of June temperature of each plot, classified by vegetation zone. The black solid line is the linear regression fitted to the correlation coefficients. The red line and number indicate where the regression line crosses zero, i.e., the temperature at which the correlation coefficients change sign. Pearson's correlation coefficient ( $r$ ) is also displayed. Abbreviations:  $T_{\max}$  = 99th percentile of maximum daily temperature ( $^{\circ}\text{C}$ ) in a month; VPD = mean daily water vapor pressure deficit (kPa) in a month;  $T_{\text{avg}}$  = mean daily average temperature ( $^{\circ}\text{C}$ ) in a month; GlobR = mean daily global radiation intensity ( $\text{kJ m}^{-2} \text{day}^{-1}$ ) in a month;  $\text{SPI}_{1\text{-month}}$  = standardised precipitation index based on total monthly precipitation (mm/month).

Rosner et al., 2018). On average, the fastest radial growth rate occurs in late June and early July across Finland, coinciding with the highest daily temperatures of the summer (Mäkinen et al., 2003; Kalliokoski et al., 2012; Jyske et al., 2014). Consistent with these findings, Schmitt et al. (2004) observed the highest radial growth rate in the northern boreal zone between the fourth week of June and the second week of July.

Several previous studies have shown that growth variation of spruce in central and northern Fennoscandia is mainly related to current summer temperature (e.g., Mäkinen et al., 2000; Merlin et al., 2024), but in central Europe high temperatures are negatively correlated with radial increment (Mäkinen et al., 2002; Lévesque et al., 2013). This study corroborates these results, showing that high June temperatures promote tree growth at northern latitudes and the growth response to precipitation is weak. However, we found a clear south-north trend in the magnitude and sign of the correlation coefficients, with the limiting effect of low temperatures decreasing with decreasing latitude (cf., Helama et al., 2005; Ruiz-Pérez and Vico, 2020; Merlin et al., 2024). The

results revealed that warm summers are detrimental to spruce growth in southern and central Finland, i.e., the correlation coefficients with June temperature were negative. Such a consistent negative effect has not previously been found throughout southern and central Finland. The shift from temperature-limited to precipitation-limited radial growth occurred at an average June temperature of approximately  $13^{\circ}\text{C}$  in the middle boreal zone. This finding is similar to the change observed by Merlin et al. (2024) in Norway, which occurred at  $12^{\circ}\text{C}$ . However, it must be noticed that only a third of the sample trees showed a significant correlation with June temperature.

The results suggest that, beyond temperature, high summer precipitation promotes spruce growth and that drought may limit growth in the southern and central regions of the country. These findings align with earlier observations by Henttonen (1990) and Mielikäinen et al. (1996), who demonstrated a relationship between spruce growth variation in southern Finland and both temperature and precipitation. There are indications that summer drought reduces tree growth in southern

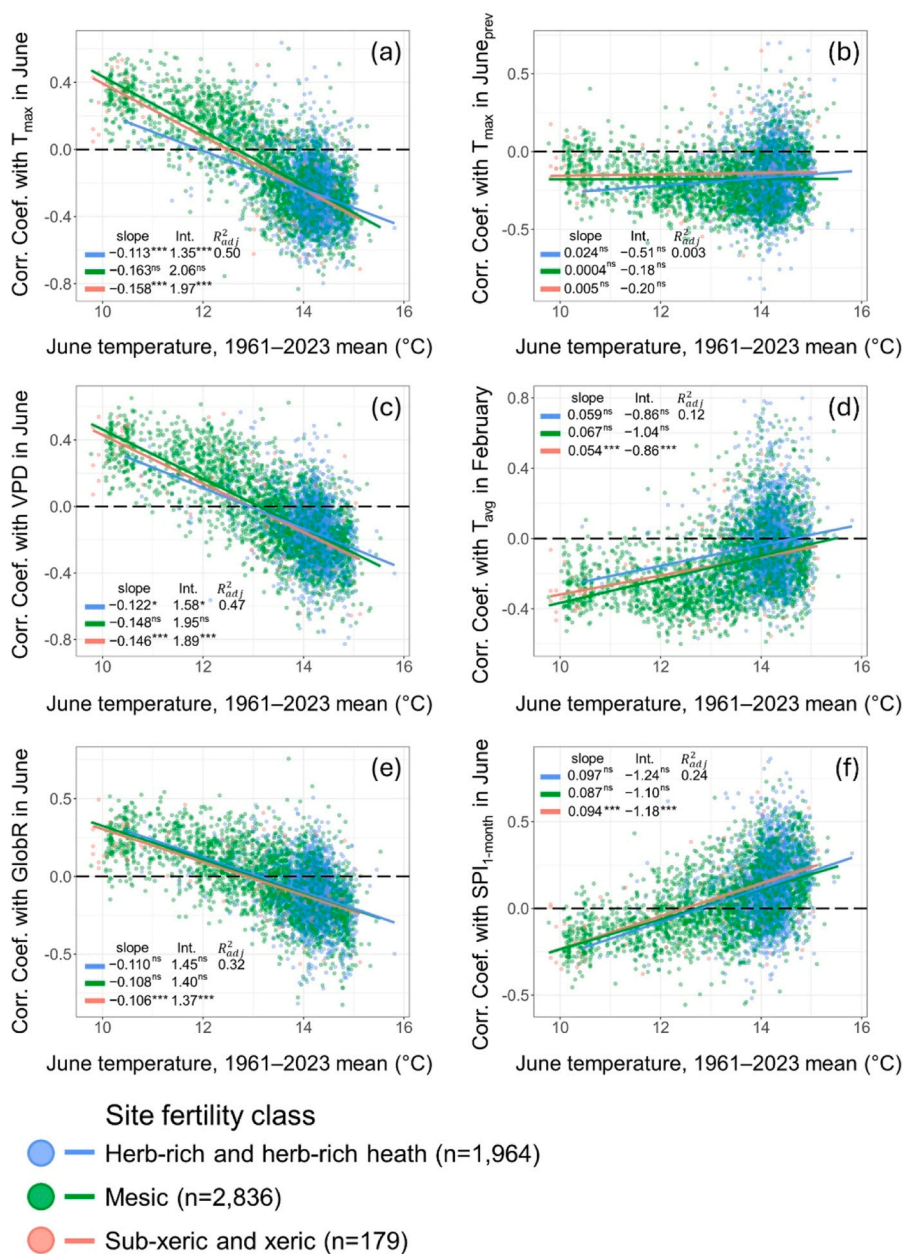


**Fig. 6.** Spearman's rank correlation coefficients between the top six weather variables and the ring-width indices (RWIs) of individual trees, plotted against the long-term mean June temperature (1961–2023). The blue, green and red solid lines are linear regressions fitted to the correlation coefficients by site fertility class. The slope and intercept (Int.) are the parameter estimates of the fit, along with the coefficient of determination ( $R^2$ ). The sub-xeric and xeric sites were used as a baseline, with dummy variables separating the herb-rich and herb-rich heath sites, as well as the mesic sites, from it. The asterisks after the intercept and slope of the sub-xeric and xeric sites indicate the statistical significance of the baseline. After the other fertility classes, asterisks indicate whether they differ from the baseline (\*\*\*) means  $p < 0.001$ ; \*\* means  $0.001 \leq p < 0.01$ ; \* means  $0.01 \leq p < 0.05$ ; ns means  $p \geq 0.05$ ). Abbreviations:  $T_{max}$  = 99th percentile of maximum daily temperature ( $^{\circ}\text{C}$ ) in a month; VPD = mean daily water vapor pressure deficit (kPa) in a month;  $T_{avg}$  = mean daily average temperature ( $^{\circ}\text{C}$ ) in a month; GlobR = mean daily global radiation intensity ( $\text{kJ m}^{-2} \text{day}^{-1}$ ) in a month;  $\text{SPI}_{1\text{-month}}$  = standardised precipitation index based on total monthly precipitation (mm/month).

Finland. For example, Kalliokoski et al. (2012) observed an early termination of spruce radial increment in southern Finland during the exceptionally dry summer of 2006. Low precipitation may also be related to spruce damage and death in sites sensitive to drought in southern Finland (Mäkinen et al., 2001).

Mäkinen et al. (2002) investigated the relationship between weather conditions and spruce growth across a geographical gradient ranging from northern Fennoscandia to central Europe. They found that, at southern sites, precipitation was a more important factor than temperature. Accordingly, a significant relationship has been observed between summer precipitation and growth variation in southern Finland and

Estonia, the correlations being higher in the southern part of the gradient (Henttonen et al., 2014). In previous studies, Mäkinen et al. (2002) and Henttonen et al. (2014) concluded that southern Finland is a transition zone where precipitation affects growth, but mainly on drought-sensitive sites. However, the current study challenges these conclusions, suggesting that water availability during the summer is the primary factor limiting spruce growth in southern Finland, but also in central Finland. Furthermore, no differences were found among site fertility classes regarding the relationship between summer precipitation and growth variation. It is difficult to find a plausible physiological explanation for this consistent relationship, as site fertility classes are

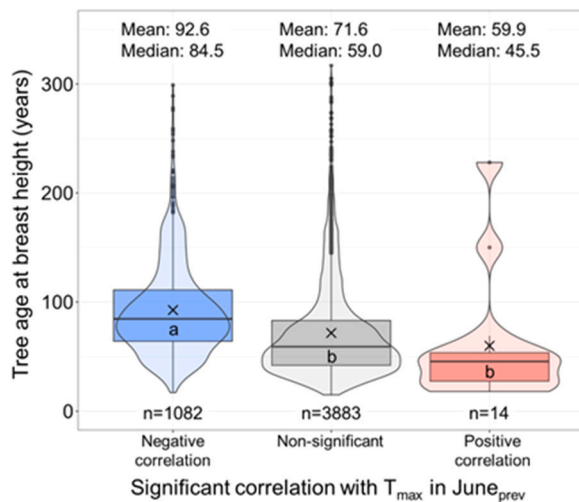


**Fig. 7.** Box and violin plots showing tree age at breast height according to the significance of the Spearman's rank correlation coefficient ( $\rho$ ) ( $p < 0.05$ ) between the ring-width indices (RWI) and the maximum daily temperature in June of the previous year. Sample sizes ( $n$ ) are shown for each group, as well as the mean and median values. Outliers are indicated by dots and the boxplots display the median, the interquartile range (IQR), and the whiskers ( $1.5 \times$  IQR rule). The  $\times$  mark denotes the mean value. Different letters indicate statistically significant differences between the groups, as determined by Duncan's multiple range test ( $\alpha = 0.05$ ).

related not only to nutrient availability, but also to soil water retention capacity.

In northern regions and at high altitudes, evapotranspiration is generally lower than precipitation, making droughts unlikely. In more southern regions, however, high temperatures can contribute to drought stress by reducing soil moisture through evapotranspiration. Reduced growth during and after droughts is caused by a decreased supply of carbohydrates resulting from reduced photosynthesis and cavitation (Eilmann and Rigling, 2012; Wiley and Helliker, 2012; Palacio et al., 2014).

Spruce growth negatively responded to high winter temperatures (cf., Helama and Sutinen, 2016; Suvanto et al., 2016; Mäkinen et al., 2022). Andreassen et al. (2006) also found that high temperatures in February were negatively related to radial growth in northern Norway and at high altitudes in south-eastern Norway. They suggested that mild winter temperatures result in an earlier break of the dormant phase, thus increasing the risk of frost damage. Spruce trees rapidly regain the potential for photosynthetic activity when temperatures increase during the cold months, making them susceptible to frost damage (Linkosalo et al., 2014). Additionally, the timing of snowmelt can affect the onset and duration of wood formation (Vaganov et al., 1999; Rossi et al., 2011; Helama et al., 2013). High winter temperatures are associated with higher precipitation, which in Finland is usually snow. A high snowpack can delay the thawing of soil frost in the spring and the subsequent increase in topsoil temperatures, affecting root metabolism and nutrient uptake (Lupi et al., 2012).

As reported in previous studies (e.g., Bouriaud et al., 2024; Merlin et al., 2024), a carry-over effect of environmental conditions in the previous year on radial growth in the current year was found. In contrast to the relationship between current-year June temperatures and radial growth, high June temperatures in the previous year were negatively related to radial growth across the country as a whole. One potential explanation for this is that warm summers promote flowering and seed production the following summer, a process requiring large quantities of photosynthetic products (Despland and Houle, 1997; Tumajer and Lehejček, 2019). The higher average age of trees with a negative correlation to previous summer temperatures supports the assumption that

cone production may play a role. The proportion of resources allocated to reproduction rather than growth varies by tree species, ranging from 10% to 20% (Ovington, 1961; Linder and Troeng, 1981; Cannell, 1985). Flowering and seed production also impact spruce volume growth by a similar magnitude (Pukkala, 1987). Radial growth reduction in masting years of high seed production has reached 50% (Selås et al., 2002). In addition to cone production, reduced radial growth the following year may also be due to a water deficit during the previous summer (Liang et al., 2013; Winkler and Oberhuber, 2017).

In previous studies, indices of individual trees were averaged over larger regions, such as biogeographic zones or NFI sampling regions (Henttonen et al., 2014, 2017). However, the NFI data exhibit large heterogeneity with respect to latitude, longitude and altitude. Calculating average indices may result in reduced variability in regional RWI time series (Sceicz and Macdonald, 1994). Consequently, the climatic signal in tree-ring chronologies may be smoothed out, causing weaker signals to be diluted or even cancelled out. Consequently, regional mean chronologies tend to highlight only the strongest climatic drivers, whereas tree-level analyses can detect subtler relationships that are masked by aggregation. This may explain why the results of this study appear stronger and more nuanced than those of the previous studies.

## 5. Conclusions

Understanding the relationship between weather variation and forest productivity is essential for predicting how boreal forests will respond to a changing climate. This large-scale analysis revealed that the anticipated benefits of higher temperatures could be diminished or negated by lower soil moisture availability. Temperature-induced water stress already appears to limit spruce growth more severely and over a larger region than expected. Therefore, it is likely that global warming will reduce spruce growth by causing more frequent and severe droughts. However, these effects are not uniform and vary according to thermal and moisture gradients. In the northernmost, cooler and wetter locations, warmer temperatures could increase the productivity of spruce forests. We therefore recommend that forest owners and policymakers apply adaptive management strategies that consider how different tree species perform and survive in a changing climate.

## CRedit authorship contribution statement

**Mäkinen Harri:** Writing – review & editing, Writing – original draft, Supervision, Project administration, Methodology, Funding acquisition, Conceptualization. **Olli-Pekka Tikkasalo:** Writing – review & editing, Writing – original draft, Validation, Software, Methodology, Data curation. **Helena Haakana:** Writing – review & editing, Writing – original draft, Visualization, Software, Resources, Methodology, Investigation, Data curation. **Daesung Lee:** Writing – review & editing, Writing – original draft, Visualization, Validation, Software, Methodology, Formal analysis.

## Funding

This research was funded by the Natural Resources Institute Finland (LUKE) strategic funded project "KuivaKuusi". The study was also supported by the Research Council of Finland (grant No 355268).

## Declaration of Competing Interest

The authors declare the following financial interests/personal relationships which may be considered as potential competing interests: Given his role as an editor of *Forest Ecology and Management*, Harri Mäkinen had no involvement in the peer-review of this article and has no access to information regarding its peer-review. Full responsibility for the editorial process for this article was delegated to another journal editor. The other authors declare that they have no known competing financial interests

or personal relationships that could have appeared to influence the work reported in this paper.

## Acknowledgements

The study was conducted at Natural Resources Institute Finland (Luke). It was supported by grants from the Research Council of Finland (Nos 348014 and 355268). We thank the NFI staff for their invaluable efforts in the fieldwork and for making the data available.

## Appendix A. Supporting information

Supplementary data associated with this article can be found in the online version at [doi:10.1016/j.foreco.2026.123967](https://doi.org/10.1016/j.foreco.2026.123967).

## Data availability

Data will be made available on request.

## References

- Adams, J. 2017. climate\_indices: An open-source Python library providing reference implementations of commonly used climate indices. GitHub repository. ([https://github.com/monocongo/climate\\_indices](https://github.com/monocongo/climate_indices)).
- Ahti, T., Hämet-Ahti, L., Jalas, J., 1968. Vegetation zones and their sections in northwestern Europe. *Acta Bot. Fenn.* 5, 169–211. (<https://www.jstor.org/stable/23724233>).
- Aldea, J., Dahlgren, J., Holmström, E., Löf, M., 2023. Current and future drought vulnerability for three dominant boreal tree species. *Glob. Change Biol.* 30. <https://doi.org/10.1111/gcb.17079>.
- Allen, C.D., Breshears, D.D., McDowell, N.G., 2015. On underestimation of global vulnerability to tree mortality and forest die-off from hotter drought in the Anthropocene. *Ecosphere* 6 (8), art129. <https://doi.org/10.1890/ES15-00203.1>.
- Andreasen, K., Solberg, S., Tveito, O.E., Lystad, S.L., 2006. Regional differences in climatic responses of Norway spruce (*Picea abies* L. Karst) growth in Norway. *For. Ecol. Manag.* 222, 211–221. <https://doi.org/10.1016/j.foreco.2005.10.029>.
- Bitterlich, W., 1984. Relascope idea: relative measurements in forestry. Commonwealth Agricultural Bureaux, Slough, U.K.
- Bouriaud, O., Frank, D., Bhatti, J.S., 2024. Assessing the influence of climate–water table interactions on jack pine and black spruce productivity in western central Canada. *Ecoscience* 21, 315–326. [https://doi.org/10.2980/21-\(3-4\)-3707](https://doi.org/10.2980/21-(3-4)-3707).
- Bunn, A.G., 2008. A dendrochronology program library in R (dplR). *Dendrochronologia* 26, 115–124. <https://doi.org/10.1016/j.dendro.2008.01.002>.
- Bunn, A., Korpela, M., Biondi, F., Campelo, F., Merian, P., Qeadan, F., Zang, C., Buras, A., Cecile, A., Mudelsee, M., Schulz, M., Klesse, S., Frank, D., Visser, R., Cook, E., Anchukaitis, K. 2025. dplR: Dendrochronology Program Library in R. (<https://github.com/OpenDendro/dplR>).
- Cannell, M.G.R., 1985. Dry matter partitioning in tree crops. In: Cannell, M.G.R., Jackson, J.E. (Eds.), *Attributes of trees as crop plants*. Institute of Terrestrial Ecology, Huntingdon, UK, pp. 160–194.
- Despland, E., Houle, G., 1997. Climate influences on growth and reproduction of *Pinus banksiana* (Pinaceae) at the limit of the species distribution in eastern North America. *Am. J. Bot.* 84, 928–937. <https://doi.org/10.2307/2446283>.
- Eilmann, B., Rigling, A., 2012. Tree-growth analyses to estimate tree species' drought tolerance. *Tree Physiol.* 32, 178–187. <https://doi.org/10.1093/treephys/tps004>.
- Fleischer, P., Pichler, V., Merganič, J., Gömöryová, E., Homolák, M., Fleischer, P. Jr., 2022. Declining growth response of Siberian spruce to climate variability on the taiga–tundra border in the Putorana mountains (Northwest Siberia). *Forests* 13, 131. <https://doi.org/10.3390/f13010131>.
- Helama, S., Lindholm, M., Meriläinen, J., Timonen, M., Eronen, M., 2005. Multicentennial ring-width chronologies of Scots pine along a North–South gradient across Finland. *Tree-Ring Res.* 61, 21–32. <https://doi.org/10.3959/1536-1098-61.1.21>.
- Helama, S., Mielikäinen, K., Timonen, M., Herva, H., Tuomenvirta, H., Venäläinen, A., 2013. Regional climatic signals in Scots pine growth with insights into snow and soil associations. *Dendrobiology* 70, 27–34. <https://doi.org/10.12657/denbio.070.003>.
- Helama, S., Sutinen, R., 2016. Inter- and intra-seasonal effects of temperature variation on radial growth of alpine treeline Norway spruce. *J. Mt. Sci.* 13, 1–12. <https://doi.org/10.1007/s11629-015-3665-9>.
- Henttonen, H. 1990. Variation in the diameter growth of Norway spruce in southern Finland (in Finnish with English summary). University of Helsinki, Finland.
- Henttonen, H.M., Mäkinen, H., Heiskanen, J., Peltoniemi, M., Laurén, A., Hordo, M., 2014. Response of radial increment variation of Scots pine to temperature, precipitation and soil water content along a latitudinal gradient across Finland and Estonia. *Agr. For. Meteorol.* 198–199, 294–308. <https://doi.org/10.1016/j.agrformet.2014.09.004>.
- Henttonen, H.M., Nöjd, P., Mäkinen, H., 2017. Environment-induced growth changes in the Finnish forests during 1971–2010 – An analysis based on National Forest Inventory. *For. Ecol. Manag.* 386, 22–36. <https://doi.org/10.1016/j.foreco.2016.11.044>.
- Hotanen, J.-P., Nousiainen, H., Mäkipää, R., Reinikainen, A., Tonteri, T. 2008. Metsätyypit - opas kasvupaikkojen luokitteluun [Forest types – a guide to site classification]. *Metsäkustannus*, 192 s.
- Jyske, T., Hölttä, T., Mäkinen, H., Nöjd, P., Lumme, I., Spiecker, H., 2010. The effect of artificially induced drought on radial increment and wood properties of Norway spruce. *Tree Physiol.* 30, 103–115. <https://doi.org/10.1093/treephys/tpp099>.
- Jyske, T., Mäkinen, H., Kalliokoski, T., Nöjd, P., 2014. Intra-annual tracheid production of Norway spruce and Scots pine across a latitudinal gradient in Finland. *Agric. For. Meteorol.* 194, 241–254. <https://doi.org/10.1016/j.agrformet.2014.04.015>.
- Kalliokoski, T., Reza, M., Jyske, T., Mäkinen, H., Nöjd, P., 2012. Intra-annual tracheid formation of Norway spruce provenances in southern Finland. *Trees* 26, 543–555. <https://doi.org/10.1007/s00468-011-0616-0>.
- Kellomäki, S., Strandman, H., Heinonen, T., Asikainen, A., Venäläinen, A., Peltola, H., 2018. Temporal and spatial change in diameter growth of boreal Scots pine, Norway spruce, and birch under recent-generation (CMP15) global climate change projections for the 21st century. *For. 9 Artic. id 118*. <https://doi.org/10.3390/f9030118>.
- Klesse, S., DeRose, R.J., Guiterman, C.H., Lynch, A.M., O'Connor, C.D., Shaw, J.D., Evans, M.E.K., 2018. Sampling bias overestimates climate change impacts on forest growth in the southwestern United States. *Nat. Commun.* 9 Artic. id 5336. <https://doi.org/10.1038/s41467-018-07800-y>.
- Korhonen, K.T., Ahola, A., Heikkinen, J., Henttonen, H., Hotanen, J.-P., Ihalainen, A., Melin, M., Pitkänen, J., Rätty, M., Sirviö, M., Strandström, M., 2021. Forests of Finland 2014–2018 and their development 1921–2018. *Silva Fenn.* 55. <https://doi.org/10.14214/sf.10662>.
- Korhonen, K.T., Ihalainen, A., Ahola, A., Heikkinen, J., Henttonen, H.M., Hotanen, J.-P., Nevalainen, S., Pitkänen, J., Strandström, M., Viiri, H., 2017. Suomen metsät 2009–2013 ja niiden kehitys 1921–2013. [Forests of Finland 2008–2013 and their development in 1921–2013]. *Nat. Resour. Bioeconomy Stud.* (<http://urn.fi/URN:ISBN:978-952-326-467-0>).
- Korhonen, K.T., Rätty, M., Haakana, H., Heikkinen, J., Hotanen, J.-P., Kuronen, M., Pitkänen, J., 2024. Forests of Finland 2019–2023 and their development 1921–2023. *Silva Fenn.* 58, 47. <https://doi.org/10.14214/sf.24045>.
- Korpela, M., Nöjd, P., Hollmén, J., Mäkinen, H., Sulka, M., Hari, P., 2011. Photosynthesis, temperature and radial growth of Scots pine in northern Finland – identifying the influential time intervals. *Trees* 25, 323–332. <https://doi.org/10.1007/s00468-010-0508-8>.
- Laudon, H., Mensah, A.A., Fridman, J., Näsholm, T., Jämtgård, S., 2024. Perspectives: Swedish forest growth decline: A consequence of climate warming? *For. Ecol. Manag.* 565, 122052. <https://doi.org/10.1016/j.foreco.2024.122052>.
- Lehto, J., Leikola, M., 1987. Käytännön metsätyypit. 4. uudistettu painos. Kirjayhtymä, Helsinki.
- Lévesque, M., Saurer, M., Siegwolf, R., Eilmann, B., Brang, P., Bugmann, H., Rigling, A., 2013. Drought response of five conifer species under contrasting water availability suggests high vulnerability of Norway spruce and European larch. *Glob. Change Biol.* 19, 3184–3199. <https://doi.org/10.1111/gcb.12268>.
- Liang, W., Heinrich, I., Simard, S., Helle, G., Liñán, I.D., Heinken, T., 2013. Climate signals derived from cell anatomy of Scots pine in NE Germany. *Tree Physiol.* 33, 833–844. <https://doi.org/10.1093/treephys/tps059>.
- Lidskog, R., Sjödin, D., 2014. Why do forest owners fail to heed warnings? Conflicting risk evaluations made by the Swedish forest agency and forest owners. *Scand. J. For. Res.* 29, 275–282. <https://doi.org/10.1080/02827581.2014.910268>.
- Linder, S., Troeng, E., 1981. The seasonal course of respiration and photosynthesis in strobili of Scots pine. *For. Sci.* 27, 267–276. <https://doi.org/10.1093/forestscience/27.2.267>.
- Linkosalo, T., Heikkinen, J., Pulkkinen, P., Mäkipää, R., 2014. Fluorescence measurements show stronger cold inhibition of photosynthetic light reactions in Scots pine compared to Norway spruce as well as during spring compared to autumn. *Front. Plant. Sci.* 5 Artic. id 264. <https://doi.org/10.3389/fpls.2014.00264>.
- Lodin, I., Brukas, V., Wallin, I., 2017. Spruce or not? Contextual and altitudinal drivers behind the choice of tree species in southern Sweden. *For. Policy Econ.* 83, 191–198. <https://doi.org/10.1016/j.forpol.2016.11.010>.
- Lupi, C., Morin, H., Deslauriers, A., Rossi, S., Houle, D., 2012. Increasing nitrogen availability and soil temperature: effects on xylem phenology and anatomy of mature black spruce. *Can. J. For. Res.* 42, 1277–1288. <https://doi.org/10.1139/x2012-055>.
- Mäkinen, H., Nöjd, P., Helama, S., 2022. Recent unexpected decline of forest growth in North Finland: examining tree-ring, climatic and reproduction data. *Silva Fenn.* 56 Artic. id 10769. <https://doi.org/10.14214/sf.10769>.
- Mäkinen, H., Nöjd, P., Mielikäinen, K., 2000. Climatic signal in annual growth variation of Norway spruce (*Picea abies* (L.) Karst.) along a transect from central Finland to Arctic timberline. *Can. J. For. Res.* 30, 769–777. <https://doi.org/10.1139/x00-005>.
- Mäkinen, H., Nöjd, P., Mielikäinen, K., 2001. Climatic signal in annual growth variation in damaged and healthy stands of Norway spruce (*Picea abies* (L.) Karst.) in southern Finland. *Trees* 15, 177–185. <https://doi.org/10.1007/s004680100089>.
- Mäkinen, H., Nöjd, P., Saranpää, P., 2003. Seasonal changes in stem radius and production of new tracheids in Norway spruce. *Tree Physiol.* 23, 959–968. <https://doi.org/10.1093/treephys/23.14.959>.
- Mäkinen, H., Nöjd, P., Kahle, H.-P., Neumann, U., Tveite, B., Mielikäinen, K., Röhle, H., Spiecker, H., 2002. Climatic response of radial growth of Norway spruce (*Picea abies* (L.) Karst.) across latitudinal and altitudinal gradients in central and northern Europe. *For. Ecol. Manag.* 171, 243–259. [https://doi.org/10.1016/S0378-1127\(01\)00786-1](https://doi.org/10.1016/S0378-1127(01)00786-1).
- Matkala, L., Kulmala, L., Kolari, P., Aurela, M., Bäck, J., 2021. Resilience of subarctic Scots pine and Norway spruce forests to extreme weather events. *Agr. For. Meteorol.* 296 Artic. id, 108239. <https://doi.org/10.1016/j.agrformet.2020.108239>.

- Mauer, O., Bagár, R., Palátová, E., 2008. Response of the Norway spruce (*Picea abies* [L.] Karst.) root system to changing humidity and temperature conditions of the site. *J. For. Sci.* 54, 245–254. <https://doi.org/10.17221/14/2008-JFS>.
- Merlin, M., Hysten, G., Vergarechea, M., Bright, R.M., Eisner, S., Solberg, S., 2024. Climate-growth relationships for Norway spruce and Scots pine remained relatively stable in Norway over the past 60 years despite significant warming trends. *For. Ecol. Manag.* 569. <https://doi.org/10.1016/j.foreco.2024.122180>.
- Mielikäinen, K., Timonen, M., Nöjd, P., 1996. Männyn ja kuusen kasvun vaihtelu Suomessa 1964–1993. [Growth variation of Scots pine and Norway spruce in Finland 1964–1993] (in Finnish). *Folia* 1996, 309–320. (<https://urn.fi/URN:NBN:fi-fe2018072333059>).
- Nevalainen, S., Matala, J., Korhonen, K.T., Ihalainen, A., Nikula, A., 2016. Moose damage in National Forest Inventories (1986–2008) in Finland. *Silva Fenn.* 50. <https://doi.org/10.14214/sf.1410>.
- Ovington, J.D., 1961. Some aspect of energy flow in plantations of *Pinus sylvestris*. *Ann. Bot.* 25, 12–20. <https://doi.org/10.1093/oxfordjournals.aob.a083728>.
- Palacio, S., Hoch, G., Sala, A., Körner, C., Millard, P., 2014. Does carbon storage limit tree growth? *N. Phytol.* 201, 1096–1100. <https://doi.org/10.1111/nph.12602>.
- Pukkala, T., 1987. Effect of seed production on the annual growth of *Picea abies* and *Pinus sylvestris*. (in Finnish with English summary). *Silva Fenn.* 21, 145–158. <https://doi.org/10.14214/sf.a15469>.
- Rosner, S., Gierlinger, N., Klepsch, M., Karlsson, B., Evans, R., Lundqvist, S.-O., Světlík, J., Borja, I., Dalsgaard, L., Andreassen, K., Solberg, S., Jansen, S., 2018. Hydraulic and mechanical dysfunction of Norway spruce sapwood due to extreme summer drought in Scandinavia. *For. Ecol. Manag.* 409, 527–540. <https://doi.org/10.1016/j.foreco.2017.11.051>.
- Rossi, S., Morin, H., Deslauriers, A., 2011. Multi-scale influence of snowmelt on xylogenesis of black spruce. *Antarct. Alp. Res.* 43, 457–464. <https://doi.org/10.1657/1938-4246-43.3.457>.
- Ruiz-Pérez, G., Vico, G., 2020. Effects of temperature and water availability on northern European boreal forests. *Front. For. Glob. Change* 3, 34. <https://doi.org/10.3389/ffgc.2020.00034>.
- Ruosteenoja, K., Markkanen, T., Räisänen, J., 2020. Thermal seasons in northern Europe in projected future climate. *Int. J. Climatol.* 40, 4444–4462.
- Salminen, H., Jalkanen, R., Lindholm, M., 2009. Summer temperature affects the ratio of radial and height growth of Scots pine in northern Finland. *Ann. For. Sci.* 66, 810. <https://doi.org/10.1051/forest/2009074>.
- Sceicz, J.M., Macdonald, G.M., 1994. Age-dependent tree-ring growth responses of subarctic white spruce to climate. *Can. J. For. Res.* 24, 120–132. <https://doi.org/10.1139/x94-017>.
- Schmitt, U., Jalkanen, R., Eckstein, D., 2004. Cambium dynamics of *Pinus sylvestris* and *Betula* spp. in the northern boreal forests in Finland. *Silva Fenn.* 38, 167–178. <https://doi.org/10.14214/sf.426>.
- Selås, V., Piovesan, G., Adams, J.M., Bernabei, M., 2002. Climatic factors controlling reproduction and growth of Norway spruce in southern Norway. *Can. J. For. Res.* 32, 217–225. <https://doi.org/10.1139/x01-192>.
- Serreze, M.C., Walsh, J.E., Chapin, F.S.L., Osterkamp, T., Dyrgerov, M., Romanovsky, V., Oechel, W.C., Morison, J., Zhang, T., Barry, R.G., 2000. Observational evidence of recent change in the northern high-latitude environment. *Clim. Change* 46, 159–207. <https://doi.org/10.1023/A:1005504031923>.
- Stone, R.S., Dutton, E.G., Harris, J.M., Longenecker, D., 2002. Earlier spring snowmelt in northern Alaska as an indicator of climate change. *AGU Fall Meeting Abstracts*, 10710. <https://doi.org/10.1029/2000JD000286>.
- Suvanto, S., Nöjd, P., Henttonen, H.M., Beuker, E., Mäkinen, H., 2016. Geographical patterns in the radial growth response of Norway spruce provenances to climatic variation. *Agr. For. Meteorol.* 222, 10–20. <https://doi.org/10.1016/j.agrformet.2016.03.003>.
- Tomppo, E., Heikkinen, J., Henttonen, H.M., Ihalainen, A., Katila, M., Mäkelä, H., Tuomainen, T., Vainikainen, N., 2011. Designing and conducting a forest inventory – case: 9th National Forest Inventory of Finland. In: *Managing Forest Ecosystems*, 22. Springer, Dordrecht. <https://doi.org/10.1007/978-94-007-1652-0>.
- Tumajer, J., Leheček, J., 2019. Boreal tree-rings are influenced by temperature up to two years prior to their formation: a trade-off between growth and reproduction? *Environ. Res. Lett.* 14, 124024. <https://doi.org/10.1088/1748-9326/ab5134>.
- Vaganov, E.A., Hughes, M.K., Kiryanov, A.V., Schweinguber, F.H., Silkin, P.P., 1999. Influence of snowfall and melt timing on tree growth in subarctic Eurasia. *Nature* 400, 149–151. <https://doi.org/10.1038/22087>.
- Wallgren, M., Bergström, R., Bergqvist, G., Olsson, M., 2013. Spatial distribution of browsing and tree damage by moose in young pine forests, with implications for the forest industry. *For. Ecol. Manag.* 305, 229–238. <https://doi.org/10.1016/j.foreco.2013.05.057>.
- Wiley, E., Helliker, B., 2012. A re-evaluation of carbon storage in trees lends greater support for carbon limitation to growth. *N. Phytol.* 195, 285–289. <https://doi.org/10.1111/j.1469-8137.2012.04180.x>.
- Winkler, A., Oberhuber, W., 2017. Cambial response of Norway spruce to modified carbon availability by phloem girdling. *Tree Physiol.* 37, 1527–1535. <https://doi.org/10.1093/treephys/tpx077>.